

## Insertion vs. Abstraction in the $\text{H} + \text{H}_2 \rightarrow \text{H}_2 + \text{H}$ Exchange Reaction

I. Schechter, R. Kosloff, and R. D. Levine\*

The Fritz Haber Research Center for Molecular Dynamics, The Hebrew University, Jerusalem 91904, Israel  
(Received: December 26, 1985)

At collision energies above 1 eV an insertion mechanism is shown to dominate in the hydrogen exchange reaction. The cone of acceptance for reaction is found to be made up of an inner cone (i.e., for more nearly collinear collisions) where exchange proceeds by abstraction and an outer spherical sector where the mechanism is by insertion. The cross section for reaction, computed by classical trajectories, declines at energies above ca. 1 eV due to a recrossing of the transition state after a collision with an inner hard core. Thus, while the barrier to insertion is higher, this mechanism dominates for such hot H atoms as are currently available from photodissociation. For the  $\text{H} + \text{HD}$  reaction with rotationally cold HD, the cone of acceptance about the D atom is significantly wider.

The hydrogen exchange reaction<sup>1</sup> is usually assumed to proceed via preferentially nearly collinear collisions. Recently, there has been considerable progress in the study of the dynamics of this reaction using translationally "hot" H atoms produced by photodissociation.<sup>2-4</sup> Examination of the potential energy surface for the  $\text{H}_3$  system<sup>5</sup> suggested to us that, for hot H atoms, the reaction will also proceed by insertion. By this we mean that the attacking H atom inserts between the two initially bound atoms while these two move apart to accommodate the incident atom. The transition state is then an equilateral triangle with the inserting atom at its apex. The purpose of this letter is to present the argument using the ab-initio potential energy surface<sup>5</sup> and then to demonstrate that dynamical (classical trajectory) computations lead to the same conclusion.

The most direct experimental test that we could find is as follows. For exchange reactions with HD which are not collinearly dominated, one expects that ejection of the H atom will be preferred.<sup>6,7</sup> That is, in an  $\text{X} + \text{HD}$  reaction, HD will be the preferential product. Trajectory computations for  $\text{H} + \text{HD}$  do show an HD/ $\text{H}_2$  branching ratio above unity (cf. Figure 4) for hot H atoms.

To consider the static steric requirements of simple exchange reactions it proves convenient to examine the recently introduced<sup>8</sup> "reaction surface". This representation of the potential energy hypersurface is similar to the familiar "polar" representation<sup>9</sup> with one key difference. In the usual polar plot the (old) bond distance is held constant and one plots the potential energy as a function of the distance and angle of orientation of the incident atom. The problem is that upon changing the (old) bond distance it is necessary to make a new plot and there can be significant and even qualitative changes in the shape of the resulting surface.<sup>10</sup> Hence, we proceed as follows. The old bond is placed (as in the ordinary polar plot) along the  $x$  axis. Then the incident atom is placed at a given distance (from the diatomic center of mass) and given

orientation angle with respect to the  $x$  axis. Now comes the new step: the (old) bond distance is varied until the minimal value of the potential energy is obtained. This minimal value is the one used in the plot. In other words, the plot shows the potential energy of the system when the old bond is allowed to fully adjust to the presence of the incident atom at a given distance and orientation.

One is quite familiar with the plot of the potential energy along the reaction path.<sup>9</sup> The reaction surface is essentially a generalization to two dimensions.

Figure 1 shows the results obtained in this fashion for the  $\text{H}_3$  system. Examination of the potential energy shows clearly the angle-dependent barrier to reaction, lowest for a collinear attack and rapidly increasing with angle.<sup>5,11</sup> This is one advantage of this new representation. Neither the angular shape of the barrier nor its height are evident in a standard polar plot. A second new feature is the shape of the inner core of the potential, and this is the subject of the present paper. Rather than a repulsive, impenetrable central core (or "tree trunk") of the usual polar plot, one sees that when the (old) bond distance is allowed to relax—the energy actually goes down upon insertion. All it takes is enough translation to overcome the barrier for a sideways attack. If that energy is available, insertion is clearly possible. In other words, when the attacking atom is energetically able to push apart the two originally bound atoms and insert itself, the energy is lowered. There is a barrier to insertion rather than a monotonic increase of the potential energy as the incident H atom approached  $\text{H}_2$  from the side.

To verify the proposed interpretation we show also the (old) bond distance, at the minimal potential energy, for fixed distance and orientation angle of the incident atom, Figure 1b. As is very evident, there are three quite distinct regions. About each H atom of  $\text{H}_2$  there is a cone of acceptance (with an opening angle of about  $60^\circ$ ) where the  $\text{H}_2$  bond is compressed upon the crossing of the barrier. For a sideways approach of H to  $\text{H}_2$  there is considerable extension of the H-H bond upon crossing of the barrier to reaction.

Comparing the two panels of Figure 1 (which are drawn to the same scale) shows clearly that the onset of either the compression or the elongation of the bond correlates with the crossing of the barrier to reaction. As is also evident, the two regimes remain quite distinct also well past the barrier. It should also be noted that, by symmetry, there are two equivalent, isoenergetic, configurations one where the "old" bond is short and the "new" bond long and the other one complementary to it. Hence compression corresponds to abstraction.

Finally we note another aspect suggested by the potential, Figure 1a. For the abstraction route, such trajectories which have enough energy to easily cross the barrier will proceed to hit the steeply repulsive inner core. They can therefore rebound, recross the barrier in the opposite direction, and thus end up as non-

(1) D. G. Truhlar and R. E. Wyatt, *Annu. Rev. Phys. Chem.*, **27**, 1 (1976).

(2) D. P. Gerrity and J. J. Valentini, *J. Chem. Phys.*, **79**, 5202 (1983); **81**, 1298 (1984); **82**, 1323 (1985).

(3) E. E. Marinero, C. T. Rettner, and R. N. Zare, *J. Chem. Phys.*, **80**, 4142 (1984).

(4) K. Tsukiyama, B. Katz, and R. Bersohn, *J. Chem. Phys.*, in press.

(5) B. Liu and P. Siegbahn, *J. Chem. Phys.*, **68**, 2457 (1978), with parameterization by D. G. Truhlar and C. J. Horowitz, *Ibid.*, **68**, 2466 (1978).

(6) J. T. Muckerman in *Theoretical Chemistry: Theory of Scattering*, Vol. 6A, D. Henderson, Ed., Academic Press, New York, 1981, p 1.

(7) K. Tsukiyama, B. Katz, and R. Bersohn, *J. Chem. Phys.*, **83**, 2889 (1985).

(8) A more detailed motivation and discussion of the reaction surface and additional examples will be formed in a forthcoming paper by I. Schechter, R. Kosloff, R. D. Levine, and R. B. Bernstein.

(9) See, for example, R. D. Levine and R. B. Bernstein, *Molecular Reaction Dynamics*, Clarendon Press, Oxford, 1974.

(10) I. Schechter, R. Kosloff, and R. D. Levine, *Chem. Phys. Lett.*, **121**, 297 (1985).

(11) R. N. Porter and M. Karplus, *J. Chem. Phys.*, **40**, 1105 (1964).

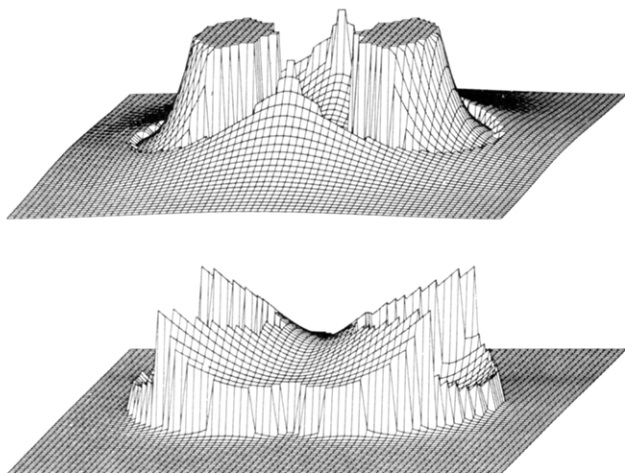


**Figure 1.** Reaction surface for the  $H_3$  system. Shown is (a, top) the minimal potential energy and (b, bottom) the H-H bond distance for a given H atom separation from the H-H center of mass and a given orientation. Both plots are on a grid of  $72 \times 72$  points (adjacent points are 0.1 au apart). In plot a the potential is truncated at 0.1 au. In plot b the vertical distance scale is such that the plateau is at the  $H_2$  equilibrium distance and the maximal value shown is 5.1 au.

reactive. Less so for sideways attack. To be sure, the barrier for reaction by insertion is higher but most of those trajectories that have enough translational energy to surmount it will not encounter a repulsive potential to be reflected by. Hence the probability for reaction is higher by the insertion mechanism at such energies (say  $>1$  eV) where the barrier is not a handicap.

The qualitative conclusions based on examination of the potential can be made quantitative by computing cross sections by the method of classical trajectories.<sup>12</sup> The initial conditions were as follows: the angle  $\theta$  between the bond direction of the molecule and initial direction of the relative velocity was confined to the range  $0$  to  $\pi/2$  (or  $\pi/2$  to  $\pi$ ) and all other initial conditions were selected as usual. For each trajectory, the value of the angle  $\gamma$  between the distance of the incident atom to the near atom of the diatomic and the bond direction (cf. Figure 2) at the point of crossing the barrier was noted. The restriction on the range of  $\theta$  means that the trajectories correspond to the incident atom approaching within a given (left or right) hemisphere and enables us to speak of the initially "near" and "far" atoms of the diatomic. There are then four possible mechanisms for an  $A + BC$  collision. (i) A approaches from the B side and abstracts to form AB. (ii) A approaches sideways and inserts to form AB. (iii) Ditto, but to form AC. (iv) A starts the collision from the B side but crosses the barrier at the C side to form AC by abstraction. Despite excellent statistics (e.g., up to 20000 trajectories at a given energy), there were practically no reactive collisions ( $<0.1\%$ ) of the fourth type. A small fraction (as shown in the figure) did react by an insertion followed by exit with the initially far atom, i.e., the third mechanism. Above ca. 1 eV (see also Figure 3) insertion tends to dominate.

We have verified that when  $\theta$  is allowed to vary over its entire range, but the definition of  $\gamma$  is carefully adhered to, the results of Figure 2 remain unchanged, as they should. Restricting the range of  $\theta$  is purely for computational convenience.

As is quite evident from the figure, the contribution of the abstraction mechanism to the reaction cross section (given by the area under the  $d\sigma/d \cos \gamma$  vs.  $\cos \gamma$  curve) declines past 1 eV, where reaction by insertion becomes the dominant mechanism. A summary of the computed energy dependence of the reaction cross section (for rotationally cold reagents) is given in Figure 3.

The classical trajectories were followed well into the exit valley so that various final state attributes could be computed. The expected differences between the two types of mechanisms could

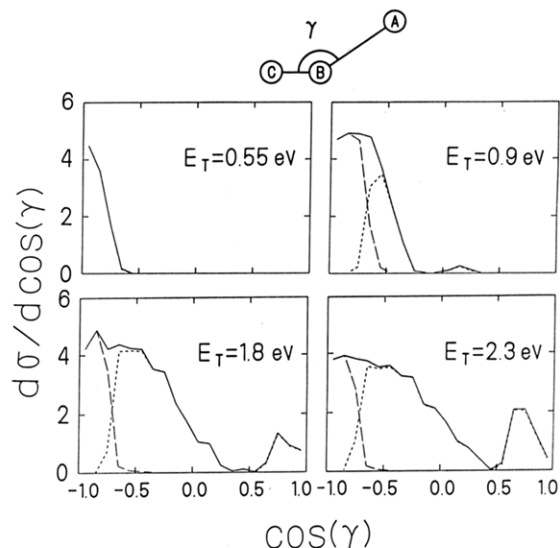


**Figure 2.** The reaction cross section (in atomic units) for the  $H +$  oriented  $D_2$  reaction.  $D_2$  is rotationally cold and in the  $v = 0$  vibrational state.  $\gamma$  is the angle of the H atom distance to the nearer D atom and the  $D_2$  bond. All the events shown correspond to trajectories such that the initial value of  $\cos \theta$  is in the interval from  $-1$  to  $0$ , where  $\theta$  is the initial angle of the  $D_2$  bond with respect to the relative velocity. In other words, all the collisions shown correspond to H approaching from the right hemisphere of  $D_2$ . The solid line is  $d\sigma/d \cos \gamma$  for all these trajectories. The contribution by those reactive collisions which proceed by abstraction is shown by the dash-dot line. At  $E_T = 0.55$  eV essentially all reactive collisions are nearly collinear.<sup>13</sup> The dashed line shows the contribution of those collisions which proceed by insertion and reaction with the "near" D atom. The dotted line is for insertion and reaction with the "far" D atom.

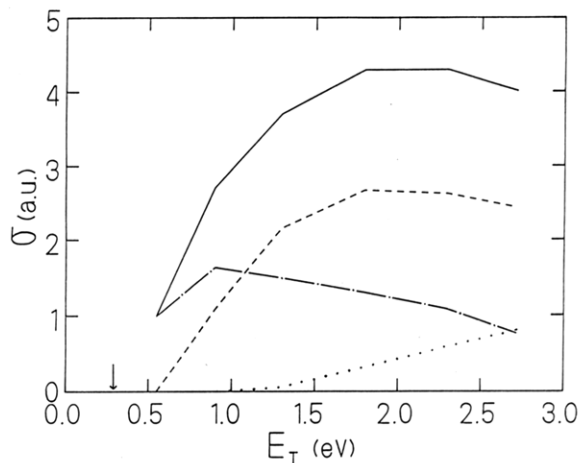


**Figure 3.** Reaction cross section for  $H + D_2$  vs. initial translational energy. All other details as in Figure 2.

all be demonstrated. For example, insertion leads to preferential sideways scattering of the products. The shift in the angular distribution for reactive scattering from backward to sideways scattering as the collision energy is increased<sup>13</sup> is thus interpreted by us as reflecting a change in the mechanism. We are so far unable, however, to provide a sharp test for an experimental demonstration of the presence of both mechanisms for homonuclear reagents. Trajectories were therefore also run for the  $H + HD$  reaction. Our result shown in Figure 4 is that, using hot H atoms, reactive formation of HD is significantly more probable than that of  $H_2$ . This is consistent with the conventional wisdom that an insertion reaction with HD will lead preferentially to an H atom ejection.

(12) N. C. Blais, R. B. Bernstein, and R. D. Levine, *J. Phys. Chem.*, **89**, 10 (1985).

(13) H. R. Mayne and J. P. Toennies, *J. Chem. Phys.*, **75**, 1794 (1981); R. Götting, H. R. Mayne, and J. P. Toennies, *J. Chem. Phys.*, **80**, 2230 (1984).

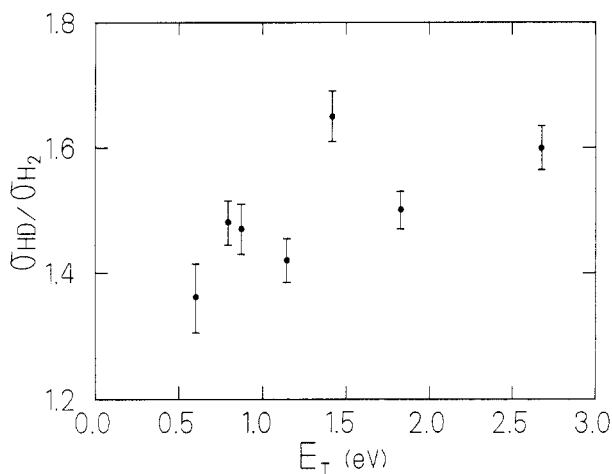


**Figure 4.** The HD/H<sub>2</sub> branching ratio in the H + HD reaction vs. the initial translational energy. The error bars are one standard deviation reflecting the finite number of trajectories (24000 per point) used.

Early experiments<sup>14,15</sup> with hot T atoms are in agreement with the trend reported in Figure 4. For T atoms produced by photolysis of DBr at 185 nm the TD/TH branching ratio is<sup>14</sup> 1.4 while it is<sup>15</sup> 1.6 for possibly hotter T atoms produced in nuclear recoil.

- (14) C. C. Chou and F. S. Rowland, *J. Chem. Phys.*, **46**, 812 (1967).  
 (15) D. Seewald and R. Wolfgang, *J. Chem. Phys.*, **46**, 1207 (1967).

A direct determination<sup>16</sup> for H + HD yields a branching ratio of  $1.87 \pm 0.1$  for H atoms with an initial kinetic energy of 2.87 eV.

Examination of a novel representation of the potential energy surface leads us to the conclusion that there is "structure" within the cone of acceptance for reaction. The implications were followed by a Monte Carlo trajectory computation. In one important respect, however, the use of classical dynamics is somewhat overconvincing. Experimentally one cannot hope to orient the reagents as well as is allowed by classical mechanics. Particularly for the lower rotational states there is a considerable (quantal) spread in the orientation even for a sharply selected  $j, m_j$  state. The features shown in Figure 1 have also been noted by us in many other systems and we are therefore looking for a simple system where the collinear and sideways attack are more sharply separated (as they apparently are<sup>17</sup> in NO + O<sub>3</sub>).

*Acknowledgment.* We thank Prof. J. J. Valentiny for discussions. This work was supported by the U.S.-Israel Binational Science Foundation (B.S.F.), Jerusalem, Israel. The Fritz Haber Research Center is supported by the Minerva Gesellschaft für die Forschung, mbH, München, BRD.

- (16) J. M. White, *Chem. Phys. Lett.*, **4**, 441 (1969).

- (17) S. Stolte, *Ber. Bunsenges. Phys. Chem.*, **86**, 413 (1982); D. van den Ende, S. Stolte, J. B. Cross, G. H. Kwei, and J. J. Valentini, *J. Chem. Phys.*, **77**, 2205 (1982).

## EPR Observation of Nitroxide Free Radicals during Thermal Decomposition of 2,4,6-Trinitrotoluene and Related Compounds

Ted M. McKinney, Leslie F. Warren, Ira B. Goldberg,\*

Rockwell International Science Center, Thousand Oaks, California 91360

and Jon T. Swanson

Frank J. Seiler Research Laboratory (AFSC), USAF Academy, Colorado Springs, Colorado 80840-6528

(Received: December 17, 1985)

Evidence is presented to support the observation by electron paramagnetic resonance (EPR) of nitroxide radicals formed by intermolecular coupling during the thermal decomposition of 2,4,6-trinitrotoluene (TNT) alone and during thermolysis of TNT in the presence of hexamethylbenzene (HMB) or perdeuteriohexamethylbenzene (HMB-*d*<sub>18</sub>). Similar results are reported for the thermal reaction of 1,3,5-trinitrobenzene (TNB) with HMB, HMB-*d*<sub>18</sub>, and TNT. A reaction mechanism is proposed. An unidentified nitroxide radical has been separated chromatographically from TNT thermolysis products.

Many of the explosives and propellants used for commercial and defense applications incorporate 2,4,6-trinitrotoluene (TNT) as a major component of the formulation. The thermal decomposition of TNT has important implications for the stability and reliability of such materials.

A number of workers have reported electron paramagnetic resonance (EPR) spectra of free radicals formed during photolysis<sup>1</sup> and thermolysis<sup>2</sup> of TNT. EPR spectra obtained during in situ thermolysis are generally characterized by low signal-to-noise ratios and varying degrees of asymmetry, indicating the presence of more

than one radical species, as shown in Figure 1a. A variety of structures have been postulated to account for the observed EPR spectra. Likewise, a panoply of diamagnetic materials have been isolated and identified from TNT photochemical<sup>3</sup> and thermolytic reactions.<sup>4</sup>

In addition to the two species clearly evident in Figure 1a (one with extensive hyperfine structure and another broad spectral line devoid of structure), we have also noted marked variations in the

- (1) (a) R. M. Guidry and L. P. Davis, *Thermochim. Acta*, **32**, 1 (1979).  
 (b) E. G. Janzen, *J. Am. Chem. Soc.*, **87**, 3531 (1965).  
 (2) L. P. Davis, J. S. Wilkes, H. L. Pugh, and K. C. Dorey, *J. Phys. Chem.*, **85**, 3505 (1981), and references therein.

- (3) (a) N. E. Burlinson, L. A. Kaplan, and C. E. Adams, NTIS Report AD-769-670, Oct 3, 1973. (b) L. A. Kaplan, N. E. Burlinson, and M. E. Sitzman, DTIC Report, NSWC/WOL/TR 75-152, Nov 21, 1975.

- (4) (a) W. P. Colman and F. P. Rausch, DTIC Contract No. DAAA21-70-0531, Feb, 1971. (b) J. C. Dacons, H. G. Adolph, and M. J. Kamlet, *J. Phys. Chem.*, **74**, 3035 (1970). (c) R. N. Rogers, *Anal. Chem.*, **39**, 730 (1967).